RESEARCH ARTICLE

Raman spectroscopy study, magnetic and microwave absorbing properties of modified barium strontium monoferrite Ba$_{(1-x)}$Sr$_{(x)}$Fe$_2$O$_4$

Ade Mulyawan[*], Wisnu Ari Adi, Yunasfi

Center for Science and Technology of Advanced Materials, National Nuclear Energy Agency of Indonesia (BATAN) Kawasan Puspiptek Serpong, Tangerang Selatan 15314, Indonesia

* Corresponding author: ademulyawan@batan.go.id
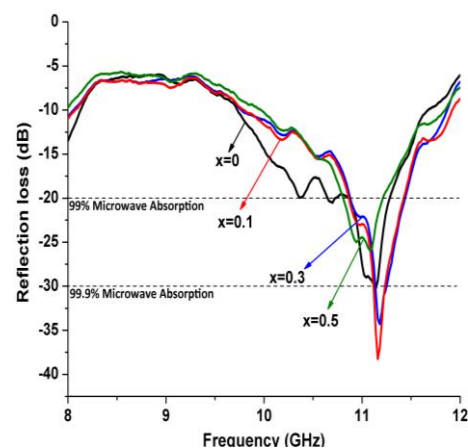
Graphical abstract

Abstract

In the contrary to other common AFe$_2$O$_4$ (A = Mn, Fe, Co, Ni, etc), Barium Monoferrite (BaFe$_2$O$_4$) have a more complex structure that exhibits orthorhombic structure. The structure of barium monoferrite permits to substitute Ba^{2+} with another divalent ion metals such as Strontium (Sr^{2+}) to improve the magnetic and microwave absorbing property. In this study, Barium Strontium Monoferrite in the form of Ba$_{(1-x)}$Sr$_{(x)}$Fe$_2$O$_4$ (0.0 $\leq$ x $\leq$ 0.5) has been successfully fabricated using high energy milling technique. Fine nanoparticle powder was characterized by using X-ray diffractometer (XRD) and Raman spectroscopy, the property of magnetic behavior and microwave absorbing were analyzed by using Vibrating sampel magnetometer (VSM) and Vector network analyzer (VNA). In the composition of x=0 and 0.1, all of the Raman spectra peaks were confirmed and matched with Raman-active vibrational modes of BaFe$_2$O$_4$ Orthorhombic structure with Space Group Cmc21 and Point Group C$_{2v}$ (mm2) that correspond to the single phase of BaFe$_2$O$_4$ according to the results of XRD. In the composition of x=0.3, the highest-frequency Raman active mode was still unaffected by the Sr^{2+} substitution whereas the lower-frequency Raman active mode were clearly changed due to the overload distortion of the Sr^{2+}.The highest-frequency Raman active mode were totally changed in the composition of x=0.5. Referring to the M-H curves, all of the compositions show a strong ferromagnetic behavior. The largest coercive force of 3285 Oe was obtained in the composition of x=0.1. A siginificant property of microwave absorbing also exhibited in the composition of x=0.1, in which the value of the reflection loss reached -38.25 dB (~99.9%) in the range of 11.2 GHz.

Keywords: Barium monoferrite, strontium modification, raman spectroscopy, magnetic properties, microwave absorbing properties

INTRODUCTION

In recent years, the use of the technology that require giga-hertz frequency range have been intensively used either in daily uses, such as for mobile phones application and communication technology, or in specific purposes, such as military application for stealth technology and radar communication (Ying *et al*., 2011; Hazra *et al.*, 2015; Shen et *al.,* 2012; Tyagi *et al*., 2011,). In contrast to the massive growth in such a wide application area, electromagnetic interference (EMI) is the phenomenon that can decrease the rapid development of the technology application by distracting the function of the electronic devices and finally causes a failure of the system. A malfunction electronic devices caused by the overexposure of the microwave energy could be potentially dangerous for human biological systems, such as affecting the heart rhythms, decreasing immune response, and also increasing the possibility of cancer (Weimo *et al.,* 2011). For specific purposes, such as for military application, erasing the unwanted electromagnetic signals become a crucial part to create stealth aircraft and camouflaging military facilities against radar detection (Cheng & Ren, 2016).

Due to the specific range frequency for military application, microwave absorbing materials worked in the frequency range of 8-12 GHz are also known as radar absorbing materials (RAM). The quality of the RAM is expected to have broad frequency range with minimum reflection loss value (RL), therefore the main concern of this typical research is to broadening the frequency range and minimize the RL value. Ferrite materials either in the spinel or hexagonal structure form are known to be a common candidate of RAM (Teber *et al*., 2017; Ghasemi *et al.,* 2009, Gunanto *et al.*, 2016). Unlike the ferrite materials, Barium Monoferrite (BaFe$_2$O$_4$) has an orthorhombic structure where the Fe^{3+} is bonded tetrahedronally with O^{2-} ions. BaFe$_2$O$_4$ is less popular compared to the spinel and hexagonal ferrite due to the assumption only as the coexisting phase along with Fe$_2$O$_3$ before turning into BaFe$_{12}$O$_{19}$ phase (Candeia *et al.*, 2007). In fact, BaFe$_2$O$_4$ exhibits several comparable properties compared to those common ferrite materials, such as high capacity of magnetization, highly stable, high coercivitiy, high permittivity, low-band-gap ferrite material that also can be used as proper candidate of RAM (Borse *et al.,* 2011). In addition, the phase formation of BaFe$_2$O$_4$ require lower temperature process compared to those common ferrites, this phenomenon can be a huge benefit in industrial process to produce

massive RAM products (Mulyawan *et al.,* 2016; Lazarević *et al.,* 2012; Li *et al*., 2012; Novizal *et al*., 2016).

Referring to the above facts and phenomena, the aim of the present work is to synthesize and modify $BaFe_2O_4$ as the candidate of RAM, which as far as the literature research by the authors have never been reported. According to the previous research, it is well known that a slight modification to the initial structure could change the magnetic and dielectric properties, which finally lead into the enhancement of the microwave absorbing property (Li *et al*., 2012; Li *et al.,* 2015). In order to improve the microwave absorbing property, the initial structure of $BaFe_2O_4$ was modified by the substitution of Barium ion (Ba^{2+}) with Strontium ion (Sr^{2+}) in the form of $Ba_{(1-x)}Sr_{(x)}Fe_2O_4$ ($0.0 \leq x \leq 0.5$). The effect of Sr^{2+} substitution to the magnetic property of the initial structure was also investigated. Raman spectroscopy is used to ensure the phase transition due to the Sr^{2+} occupation to the main structure of $BaFe_2O_4$. Raman spectroscopy compiled with X-ray diffractometer (XRD) is a powerful tool to ensure the phase transition since it is very sensitive to see the vibration of the crystal structure, so that the purity of the main phase or even the presence of secondary phases can be detected (Chen *et al*., 2010).

EXPERIMENTAL

Materials

A series of modified Barium Monoferrite by substituting Strontium (Sr^{2+}) in the form of $Ba_{(1-x)}Sr_{(x)}Fe_2O_4$ ($0.0 \leq x \leq 0.5$) have been made by using chemical compound of $BaCO_3$ (merck) , $SrCO_3$ (merck), and Fe_2O_3 (sigma Aldrich) with purity >99.5%, with the stoichiometry as follow:

$$(1-x)BaCO_3 + (x)SrCO_3 + Fe_2O_3 \rightarrow Ba_{(1-x)}Sr_{(x)}Fe_2O_4 + CO_2 \quad (1)$$
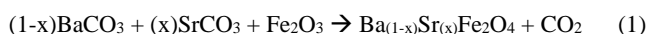
Synthesis of modified Barium Monoferrite $Ba_{(1-x)}Sr_{(x)}Fe_2O_4$

A series of $Ba_{(1-x)}Sr_{(x)}Fe_2O_4$ ($0.0 \leq x \leq 0.5$) were made by using high energy milling (HEM) technique. Each composition of $Ba_{(1-x)}Sr_{(x)}Fe_2O_4$ ($0.0 \leq x \leq 0.5$) was milled for 5 hours using HEM machine then continued to the pre-heating process at 700^0C and followed by sintering process at 900^0C for 5 hours, respectively. For further characterization, each composition was grinded by using agate mortar until fine powder was formed.

X-ray diffraction pattern of all modified Barium monoferrite samples were collected by using Panalytical Phillips (Cu Kα radiation, λ=0.15406 nm) in the range of 2Θ angles starting from 10^0 to 80^0 with scan step 0.0263^0 per second. The detailed refinement results and three dimensional crystal structure have been discussed in previous paper (Mulyawan *et al*., 2016). The characterization of Raman spectroscopy were carried out by using Bruker Senterra Raman spectroscopy with laser excitation of 785 nm in room temperature. The magnetic properties of all compositions were measured using Vibrating Sample Magnetometer (VSM) Oxford with 1 Tesla magnetization in room temperature. The microwave absorbing property was measured by using Vector Network Analysis (VNA) in the range of 8-12 GHz.

RESULTS AND DISCUSSION

X-Ray Diffraction results and phase transformation identification

All of the diffraction patterns of $Ba_{(1-x)}Sr_{(x)}Fe_2O_4$ ($0.0 \leq x \leq 0.5$) samples are shown in Fig. 1. As shown from Fig. 1, a single phase of Barium Monoferrite ($BaFe_2O_4$) structure with no trace of any secondary phases has been formed in the composition of $Ba_{(1-x)}Sr_{(x)}Fe_2O_4$ (x= 0 and 0.1) referring to the the Crytallography Open Database (COD) number 96-430-9916. $BaFe_2O_4$ have an orthorhombic structure with space group $Cmc2_1(36)$ with the most intense peak in the position of $2\Theta = 28.48\pm0.02^0$ that correspond to the (212) crystal plane. Referring to the diffraction pattern matching using Match! Software in Fig. 1, it can be seen that a slight substitution of Sr^{2+} to the initial structure of $BaFe_2O_4$ in the

composition of $Ba_{(1-x)}Sr_{(x)}Fe_2O_4$ (x=0.1) did not significantly change the phase formation, but still exhibit a weak diffraction peak in the position of $2\Theta = 32.69\pm0.02^0$ that correspond to the (020) crystal plane. A phase transition process from the initial phase clearly can be seen in the composition of $Ba_{(1-x)}Sr_{(x)}Fe_2O_4$ (x=0.3) in which the (020) crystal plane became weaker comparing to the composition of x = 0.1.
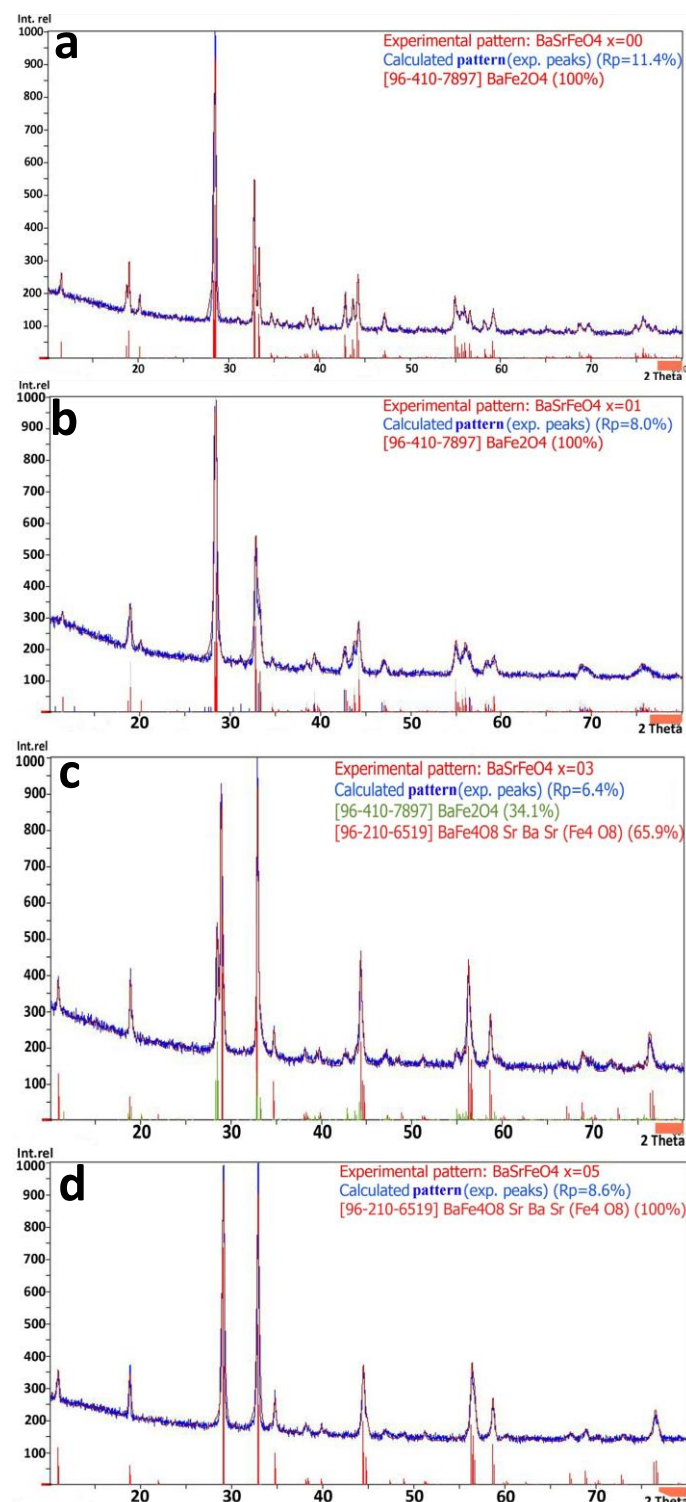

Fig. 1 X-ray diffraction patterns of all $Ba_{(1-x)}Sr_{(x)}Fe_2O_4$ compositions (a) x=0 ; (b) x=0.1; (c) x=0.3; (d) x=0.5

This phenomenon also followed by the appearance of a strong diffraction pattern in the position of $2\Theta = 32.90 \pm 0.02^0$ that correspond to the (110) crystal plane. This phenomenon indicated a clear transition process from orthorhombic to trigonal structure of $BaSrFe_4O_8$. The $BaSrFe_4O_8$ phase is known to have a trigonal

structure with space group P -3 1 m (162) with the most intense peak in the position of $2\Theta = 29.09\pm0.02^0$ and 32.90 ± 0.02^0 that correspond to the (102) and (110) crystal plane. The $BaSrFe_4O_8$ was identified using COD number 96-210-6519. A single phase of $BaSrFe_4O_8$ have fully formed In the composition of x = 0.5 with no trace of any other secondary phases.

The results of the Raman spectra for all $Ba_{(1-x)}Sr_{(x)}Fe_2O_4$ compositions are shown in Fig. 2. As far the literature research by the author, there are limited Raman spectroscopy study for a single phase of $BaFe_2O_4$ so that the assumption of total Raman-active vibrational modes can only be taken on the factor group analysis from Bilbao crystallographic server. As it is mentioned in the explanation of XRD earlier, $BaFe_2O_4$ has an orthorhombic structure with space group $Cmc2_1$ and point group C_{2v} (mm2). C_{2v} (mm2) is predicted to have 12 sets of Raman-active vibrational modes at the Γ point as shown in point 2 (Γ represents the center of Brillouin zone)

$$\Gamma = 3A_1 + 3A_2 + 3B_1 + 3B_2 \tag{2}$$
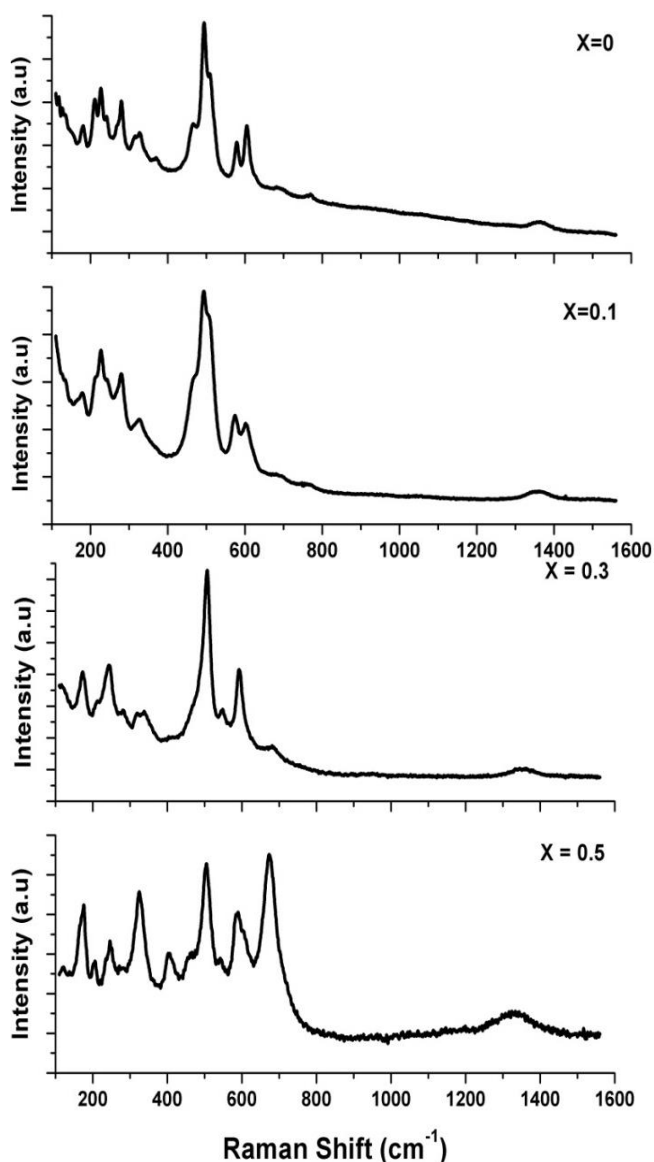
Fig. 2 Raman spectra of all $Ba_{(1-x)}Sr_{(x)}Fe_2O_4$ compositions in the range 110 cm^{-1} until 1600 cm^{-1}

Based on the results of all Raman spectra in the range 110 cm^{-1} until 1600 cm^{-1}, the results can be separated into three steps transition phase. In the first transition step, all of Raman peaks are observed in accordance with the results of the phase identification using XRD. The composition of $Ba_{(1-x)}Sr_{(x)}Fe_2O_4$ (x = 0 and 0.1) are belong to the first step in which all of the vibrational modes resembled to the Raman active modes of $BaFe_2O_4$. Several strong Raman peaks that are associated to the finger print position of the $BaFe_2O_4$ phase are located in the position of 225, 493, 602 cm^{-1}, Raman peaks in the position of 177, 209, 279,314, 461, 576, 667, 753, and 1340 cm^{-1} are also can be seen in both compositions eventhough in the composition of $Ba_{(1-x)}Sr_{(x)}Fe_2O_4$ (x = 0.1) several Raman peaks in the position of 460, 209, and 602 cm^{-1} are slightly shifted and broadened compared to the initial composition. These are associated to the asymmetry vibration of the anharmonic potential in the system (Andreasson *et al.*, 2007). The second transition step is belong to the composition of $Ba_{(1-x)}Sr_{(x)}Fe_2O_4$ (x = 0.3) in which a clear phase transition process from $BaFe_2O_4$ to $BaSrFe_4O_8$ phase can be observed. In this composition, the most intense peaks in the position around 493 and 225 cm^{-1} are still unaffected by the Sr^{2+} substitution but Raman peaks in the lower frequency are clearly changed due to the overload distortion of the Sr^{2+}. According to the Raman studies that have been done by Yang (Yang *et al.*, 2010). It is known that a lower frequency modes especially in the A-site modes are attributed to the relative motion of cations against the Oxygen bond.This phenomenon made several Raman peaks in the range below 300 cm^{-1} that related to the Ba-O band disappear along with the emerge of new Raman peak in the position of 590 cm^{-1} which correspond to the early formation of $BaSrFe_4O_8$ phase. The last step of the transition process is a single phase formation of $BaSrFe4O8$ phase in the composition of $Ba_{(1-x)}Sr_{(x)}Fe_2O_4$ (x = 0.5), the increasing content of Sr^{2+} to the initial formula caused the Raman spectra drastically changed primarily a strong enhancement in the position of 672 cm^{-1} that became the most intense Raman peaks in this composition. It also noticeable that several sharp peaks in the range below 500 cm^{-1} have been formed. These results confirmed the phase transition process from orthorhombic structure into trigonal structure and correspond with the X-ray diffraction pattern results.

Magnetic properties

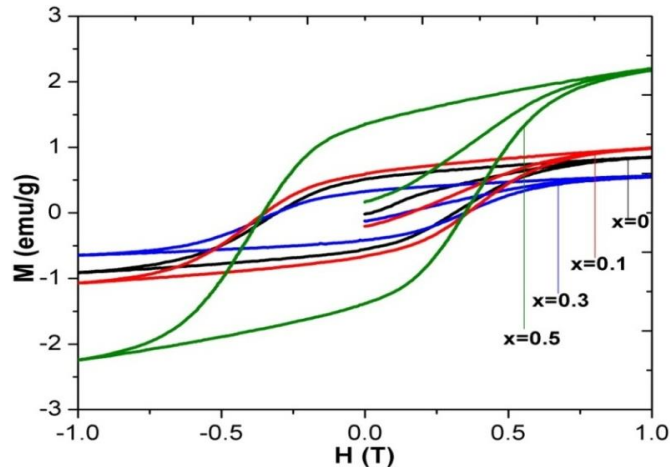The magnetization hysteresis curve of all $Ba_{(1-x)}Sr_{(x)}Fe_2O_4$ ($0.0 \leq x \leq 0.5$) are given in Fig. 3. All of the experiment results are taken in a room temperature with 1 T magnetization. The results of the magnetic properties are listed in table 1. The hysteresis curve shows that all of the modified compositions of $Ba_{(1-x)}Sr_{(x)}Fe_2O_4$ exhibit hard magnetic properties that associated to large number of the coercivity above 1000 Oe (Lamichhanne *et al.,* 2012). The saturation value (Ms) in the composition of $Ba_{(1-x)}Sr_{(x)}Fe_2O_4$ (x = 0.1) is slightly increased compared to the initial composition that attribute to the occupancy of the Sr^{2+}. In the contrary to the slight enhancement of the Ms value, the coercivity value (Hc) is highly influenced by the slight substitution of the Sr^{2+} cation. It indicates that the Alkali Sr^{2+} cation, which replacing the Ba^{2+} site in the orthorhombic structure, play an important role to originate the magnetic anisotropy and influence the domain growth and finally improved the the coercivity value (Li *et al*., 2012; Kanagaraj *et al.,* 2016). The hard magnetic properties in both compositions $Ba_{(1-x)}Sr_{(x)}Fe_2O_4$ (x = 0 and 0.1) are completely different to other common AFe_2O_4 magnetic materials that normally exhibit soft magnetic properties with a perfect 'S' shape of the Hysteresis curves (Sivakumar *et al*.,2013). This results also comparable with the study that have been done by Kanagaraj who studied the effect of Mg doped pristine Barium Nanoferrite to their magnetic properties (Kanagaraj *et al.,* 2016). In the composition of $Ba_{(1-x)}Sr_{(x)}Fe_2O_4$ (x = 0.3), the Hc value decreases along with the Ms value. It happened because the initial orthorhombic structure has reached the maximum amount of Sr^{2+} cation that could be contained in the initial orthorhombic structure and finally formed the new phase of $BaSrFe_4O_8$ that successfully distracted the coupling between Sr^{2+} cation and Fe site, thus made this composition have the lowest coercivity and magnetization saturation value. In the composition of $Ba_{(1-x)}Sr_{(x)}Fe_2O_4$ (x = 0.5), a proper coupling between Sr^{2+} cation and Fe site makes this composition have the highest Ms value of 2.05

emu/gram due to the phase formation was completely changed became the phase of BaSrFe₄O₈ without any secondary phases.

Table 1 The detailed comparison of magnetic properties for all modified composition of $Ba_{(1-x)}Sr_{(x)}Fe_2O_4$ (0.0 ≤ x ≤ 0.5)

| $Ba_{(1-x)}Sr_{(x)}Fe_2O_4$	Ms (emu/gram)	Mr (emu/gram)	Hc (Oe)
x=0	0.91	0.53	3025
x=0.1	0.97	0.61	3285
x=0.3	0.65	0.34	3150
x=0.5	2.05	1.3	3125

Fig. 3 Magnetization hysteresis curve of all modified $Ba_{(1-x)}Sr_{(x)}Fe_2O_4$ (0.0 ≤ x ≤ 0.5)

Evaluation of the Microwave absorbing properties

Referring to the transmission line theory, a microwave absorbing material properties can be determined by calculating the relative complex permeability and permittivity (Li *et al*., 2012; Zhang *et al.,* 2014). The reflection loss of electromagnetic radiation of a single layer material can be calculated by using below equation (Li *et al.,* 2012);

$$R_l = 20 log_{10} \left| \frac{z_{in} - 1}{z_{in} + 1} \right| \qquad (2)$$
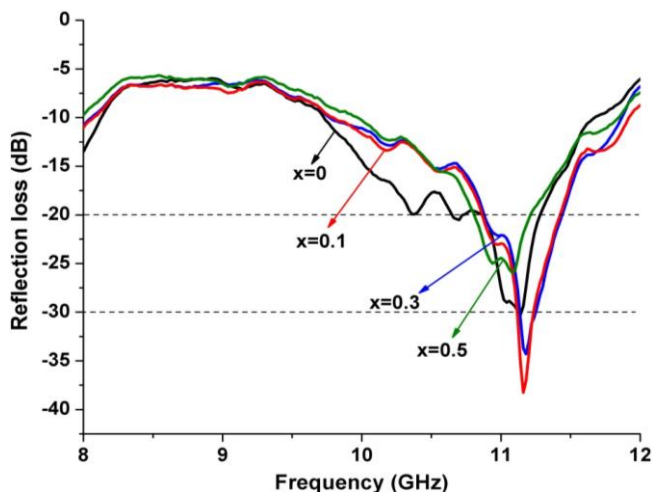
Fig. 4 Variation of the Refflection loss (RL) as a function of frequency dependences for all modified composition of $Ba_{(1-x)}Sr_{(x)}Fe_2O_4$ (0.0 ≤ x ≤ 0.5) with sample thickness of 2 mm.

Table 2 The detailed electromagnetic and microwave absorption properties for all modified composition of $Ba_{(1-x)}Sr_{(x)}Fe_2O_4$ (0.0 ≤ x ≤ 0.5) with sample thickness of 2 mm.

$Ba_{(1-x)}Sr_{(x)}Fe_2O_4$	Frequency range for RL<-20 dB (GHz)	Optimal RL (dB)	Frequency position of optimal RL (GHz)
x=0	10.85 - 11.28	-30.67	11.14
x=0.1	10.85 - 11.42	-38.25	11.16
x=0.3	10.88 - 11.44	-34.37	11.16
x=0.5	10.80 - 11.21	-25.96	11.06

Fig. 4 shows the results of RL value for all composition of $Ba_{(1-x)}Sr_{(x)}Fe_2O_4$ (0.0 ≤ x ≤ 0.5) in the range of 8-12 GHz. According to the results, all of the compositions are appropriate to be applied as a main compound of Radar absorbing material due to the RL value less than -20 dB. In the unmodified composition, there are several RL peaks which have separated broad RL curve in the frequency position of 10.34 GHz, 10.64 GHz, 11.02 GHz, and 11.14 GHz. In this composition the RL value less than -20 dB was emerged in the range of 10.85-11.28 GHz with the optimal RL value in the frequency 11.14 GHz for –30.67 dB. The composition of $Ba_{(1-x)}Sr_{(x)}Fe_2O_4$ (x=0.1) exhibit the broadest RL frequency (for frequency range <-20 dB) and the deepest optimal RL among all composition is at the value of -38.35 dB, which means in this composition is able to absorb approximately 99.9% from the initial electromagnetic wave and microwave in the frequency of 11.16 GHz, referring to the composition $Ba_{(1-x)}Sr_{(x)}Fe_2O_4$ (x=0.1) exhibited the best performance as Radar absorbing material compared to all compositions. The composition of $Ba_{(1-x)}Sr_{(x)}Fe_2O_4$ (x=0.3) reach the optimal RL value in the frequency 11.16 GHz for -34.37 dB. In the composition of $Ba_{(1-x)}Sr_{(x)}Fe_2O_4$ (x=0.5), the optimal RL value only reach -25.96 dB in the frequency 11.06 GHz.

In this study, it was known that the ability of each composition to absorp the electromagnetic and microwave is highly depend on the coercivity value. The composition of $Ba_{(1-x)}Sr_{(x)}Fe_2O_4$ (x=0.1) that showed the most prominent composition as a radar absorbing material among all compositions also have the biggest coercivity value of 3285 Oe (Table 1). As shown in Fig. 4, the separated broad RL curve of the unmodified composition (10.34 GHz, and 10.64 GHz) have disappeared in the composition of $Ba_{(1-x)}Sr_{(x)}Fe_2O_4$ (x=0.1) and made the optimal RL of this composition became deeper than the unmodified composition. From these results, it can be noticed that an appropriate modification to the initial structure of $BaFe_2O_4$ will increase an impedance matching between the materials and the initial electromagnetic and microwave and likely change the depth of the optimal RL and frequency position. These results happened due to the grain shrinkage caused by the atomic radii difference of the substitution Sr^{2+} cation that have a shorter atomic radii compared to Ba^{2+} cation (Mulyawan *et al*., 2016), the grain shrinkage obviously made the surface state and grain surface energy level changed, this finally increasing the interface polarization and more repetitious reflection of the initial microwave and electromagnetic wave so that there is more energy absorption (Li *et al*., 2012). In the composition of $Ba_{(1-x)}Sr_{(x)}Fe_2O_4$ (x=0.3), despite two phases were formed in this composition but the frequency range for RL<-20 dB was only slightly shifted compared to the composition of $Ba_{(1-x)}Sr_{(x)}Fe_2O_4$ (x=0.1). This result also related to the coercivity value in which this composition has the second largest coercivity value among all compositions. Even though in the composition of $Ba_{(1-x)}Sr_{(x)}Fe_2O_4$ (x=0.5) exhibits a bigger coercivity value compared to the unmodified composition and the biggest saturation among all compositions (table 1), it has the shallowest RL value compared to all composition. This result

attributed to the change of magneto crystalline anisotropic field that finally lead the change of the spin resonance and its natural frequency due to the fully phase transformation from $BaFe_2O_4$ with an orthorhombic structure became $BaSrFe_4O_8$ with a trigonal structure (Cheng & Ren, 2016).

CONCLUSION

In conclusion, a series of Barium Monoferrite modified by Strontium cation (Sr^{2+}) as RAM candidate in the form of

$Ba_{(1-x)}Sr_{(x)}Fe_2O_4$ ($0.0 \leq x \leq 0.5$) have been successfully synthesized by using solid state reaction method with high energy milling technique. The XRD patterns and Raman spectra show that along with the increasing Sr^{2+} substitution makes the crystal structure changed from the initial phase of $BaFe_2O_4$ that had orthorhombic structure became $BaSrFe_4O_8$ that had trigonal structure. Referring to the magnetic properties measurement using VSM, all compositions show ferromagnetic properties with the largest coercivity value belong to the composition of $Ba_{(1-x)}Sr_{(x)}Fe_2O_4$ ($x = 0.1$). This composition also exhibits the widest frequency range for reflection loss (RL) less than -20 dB with the peak value of RL in the frequency 11.16 GHz for -38.25 dB. Thus, the composition of $Ba_{(1-x)}Sr_{(x)}Fe_2O_4$ ($x = 0.1$) shows a prominent results to be applied as a main compound of RAM.

ACKNOWLEDGEMENT

REFERENCES

Liu, Y., Lian, L. X., Ye, J. (2011). Electromagnetic wave absorption properties of RE-Fe nanocomposites. In Petrin, A. (Ed.) *Wave Propagation* (pp.354-378) InTech, Available from: https://www.intechopen.com/books/wave-propagation/electromagnetic-wave-absorption-properties-of-re-fe-nanocomposites

Hazra, S., Ghosh, B. K., Patra, M. K., Jani, R. K. (2015). A novel 'one-pot' synthetic method for preparation and study of their microwave absorption and magnetic properties. *Powder Technology*. 279, 10–17.

Shen, X., Song, F., Xiang, J., Liu, M., Zhu, Y. (2012). Shape anisotropy, exchange coupling interaction and microwave absorption of hard/soft nanocomposite ferrite microfibers. *Journal of the American Ceramic Society*. 95, 3863–3870.

Tyagi, S., Baskey, H. B., Agarwala, R. C., Agarwala, V. (2011). Development of hard/soft ferrite nanocomposite for enhanced microwave absorption, *Ceramics International*. 37, 2631–2641.

Weimo, Z., Lei, W., Rui, Z., Jiawen, R., Guanzhong, L. (2011). Electromagnetic and microwave-absorbing properties of magnetic nickel ferrite nanocrystals. *Nanoscale*. 3, 2862-2864.

Cheng, Y., and Xiaohu, R. (2016). Enhanced microwave absorbing properties of La^{3+} substituting barium hexaferrite. *Journal of Superconductivity and Novel Magnetism*. 1-6.

Teber, A., Cil, K., Yilmaz, T., Eraslan, T., Uysal, D. (2017). Manganese and zinc spinel ferrites blended with multi-walled carbon nanotubes as microwave absorbing materials. *Aerospace*, 1-18.

Ghasemi, A., Sepelak, V., Liu, X., Morisako, A. (2009). Microwave absorption properties of Mn–Co–Sn doped barium ferrite nanoparticles. *IEEE Transactions on Magnetics*. 45(6), 2456-2459.

Gunanto, Y. E., Cahyadi, L., Adi, W. A. (2016). Effect of Mn and Ti substitution on the reflection loss. *AIP Conference Proceedings*. 19, 2–8.

Candeia, R. A., Souza, M. A. F., Bernardi, M. I. B., Maestrelli, S. C. 2006. Monoferrite $BaFe_2O_4$ applied as ceramic pigment. *Ceramics International*. 33, 521-525.

Borse, P. H., Cho, C. R., Lim, K. T. (2011). Synthesis of Barium Ferrite for visible light photo-catalysis applications. *Journal of the Korean Physical Society*. 6, 1672–1678.

Mulyawan, A., Adi, W., Ari., Fisli, A. (2017). The phase transformation and crystal structure studies of Strontium substituted Barium Monoferrite. *IOP Conference Series : Earth and Environmental Science*. 58,1-10.

Lazarević, Z. Ž., Jovalekić, Č., Sekulić, D., Slankamenac, M., Romčević, M. (2012). Characterization of nanostructured spinel $NiFe_2O_4$ obtained by soft mechanochemical synthesis. *Science of Sintering*. 44(3), 331–339.

Li, C. J., Bin, W., Jiao-Na, W. (2012). Magnetic and microwave absorbing properties of electrospun $Ba(1−x)LaxFe_{12}O_{19}$ nanofibers. *Journal of Magnetism and Magnetic Materials*. 324, 1305–1311.

Novizal, Manaf, A., Fajrah, M. C. (2016). The effect of induced magnetic anisotrophy on the hysteresis parameter of nano barium strontium hexaferrite prepared by mechanical alloying and sonication. *International Journal of Technology*. 3, 486–492.

Li, J. Zhang, H., Liu, Y., Li, Q., Zhou, T., Yang, H. (2015). Phase formation, magnetic properties and raman spectra of Co-Ti co-substitution M-type barium ferrites. *Applied Physics A: Materials Science and Processing*. 119(2), 525–532.

Chen, I-. H., Wang, C-. C., Chen, C-. Y. 2010. Fabrication and characterization of magnetic cobalt ferrite/polyacrylonitrile and cobalt ferrite/carbon nanofibers by electrospinning. *Carbon*. 48, 604-611.

Andreasson, J., Holmlund, J., Knee, C. S., Käll, Mikael., Börjesson, Lars. (2007). Franck-Condon higher order lattice excitations in the $LaFe1−xCrxO3$ (x=0, 0.1, 0.5, 0.9, 1.0), perovskites due to Fe-Cr charge transfer effects. *Physical Review B*. 75, 104302(1-8).

Yang, Y., Yu-Long, L., Ke, Z., Li-Yan, Z., Shu-Yuan, M. (2010). Structural Properties of $Bi_{1− x}La_XFeO_3$ Studied by micro-Raman Scattering. *Chinese Physics*. 3, 1–6.

Lamichanne, M., Rai, B. K., Mishra, S. R., Nguyen, V.V., Liu, J. P. (2012). Magnetic properties hard-soft $SmCo5-FeNi$ and $SmCo5-FeCo$ composites prepared by electroless coating technique. 2, 119–124.

Kanagaraj, M., Kokila, I. P., Subbulakshmi, N., Kumar. (2016). A systematic investigation of structural, optical and magnetic properties of pristine. *Indian journal of Pure and Applied Physics*. 54, 500–506.

Sivakumar, P., Ramesh, A., Ramanand, A., Ponnusamy, A., Muthamizhzhelvan, C. (2013). Synthesis and characterization of $NiFe_2O_4$ nanoparticles and nanorods. *Journal of Alloys and Compounds*. 563, 6–11.

Jiaoqiang, Z., Changming, S., Tiezheng, J., Guanglei, W., Kaichang, K. (2014). preparation and microwave absorbing characteristics of multi-walled carbon nanotube/chiral-polyaniline composites. *Open Journal of Polymer Chemistry*. 4, 62–72.

Jingbo, G., Yuping, D., Lidong, L., Liyang, C., Shunhua, L. (2011). Electromagnetic and microwave absorption properties of Carbonyl-Iron / Fe91Si9 composites in gigahertz range. *Journal of Electromagnetic Analysis and Applications*. 3, 140–146.